HEOS 1 HELIUM OBSERVATIONS IN THE SOLAR WIND

D. Bollea, V. Formisano, P. C. Hedgecock, G. Moreno and F. Palmiotto

ABSTRACT Results of α-particle observations performed by the European satellite HEOS 1, in the period from December 9, 1968, to April 13, 1969, and from September 6, 1969, to April 15, 1970, are presented. The average bulk velocities of protons V_p and α-particles V_α appear to be equal; however, due to an instrumental bias, the possibility of V_α being lower than V_p cannot be ruled out. Comparison with observations of Vela 3 and Explorer 34 satellites gives evidence of a dependence of helium abundance on the solar cycle. The problem of the stability of differences between the bulk velocities of protons and α-particles is investigated. The behavior of α-particles through interplanetary shock waves is illustrated in connection with magnetic field measurements.

INTRODUCTION

Initial results on the observations of the helium component of the solar wind, performed by the ESRO satellite HEOS 1, are given by *Formisano et al.* [1970*a*] and *Formisano et al.* [1970*b*]. Here we summarize the results obtained during the period from December 9, 1968, to April 13, 1969, and from September 6, 1969, to April 15, 1970. Observations of three interplanetary shock waves are presented, using HEOS 1 plasma and magnetic field data. Details of the satellite orbit, the particle detector, and the measurement routine are given by *Bonetti et al.* [1969].

HEOS 1 was launched on December 5, 1968, on a highly eccentric orbit. The satellite is spin stabilized; the spin period is ~6 sec, and the angle between spin axis and sun-satellite line is always in the range $90° \pm 20°$. The positive ion detector (consisting of a hemispherical electrostatic deflector and a Faraday cup) points perpendicular to the spin axis. Each measurement consists essentially of the positive ion flux integrated over an angle of 180° centered about the sun-satellite direction. Flux measurements are performed in 28 adjacent energy channels according to a programmed sequence, covering the range of energy per unit charge from about 200 to about 16,000 eV/Z. A complete energy distribution is obtained every 6.4 min, which is the duration of a telemetry subframe. The particular time sequence chosen for the energy channels allows a discrete-step coverage of the whole energy range in four subcycles of 1.6-min duration. The sensitivity of the instrument is approximately 10^7 protons/cm^{2}s or 5×10^6 α-particles/cm^{2}s.

The magnetic field experiment on board HEOS 1 has been described by *Hedgecock* [1970].

AVERAGE PROPERTIES

During the time period considered, α-particles were detected in 4,997 subframes, corresponding to a total observation time of ~20.8 days. The method of analysis to obtain the parameters of interest (α-particle number density N_α, bulk velocity V_α, most probable thermal speed W_α) has been described by *Bonetti et al.* [1969] and *Formisano et al.* [1970*b*].

Drs. D. Bollea, V. Formisano, and F. Palmiotto are at the Laboratorio per lo Studio del Plasma nello Spazio del C.N.R., Roma, Istituto di Fisica dell'Università, Roma. Dr. P. C. Hedgecock is at the Department of Physics, Imperial College of Science and Technology, London. Dr. G. Moreno is at the Laboratorio per le Radiazioni Extraterrestri, C.N.R., Bologna–Firenze, Cattedra di Fisica dello Spazio, Università, Firenze.

Figure 1 shows the frequency distribution of individual values of V_α/V_p (ratio of α-particle to proton bulk velocity). The average value of V_α/V_p is 1.02, identical to the value obtained by *Robbins et al.* [1970] from Vela 3 observations. Though the deviation of this value

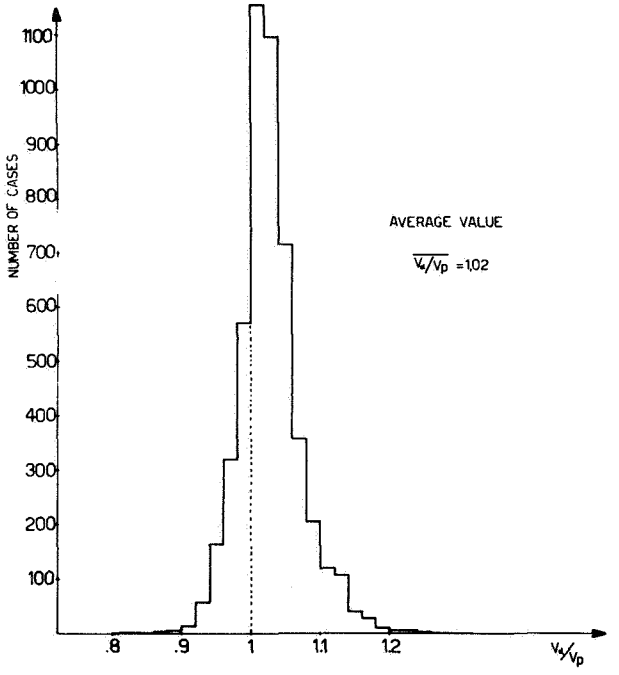

Figure 1. *Frequency distribution of individual values of V_α/V_p.*

from 1 is relatively small, attention should be paid to the lack of symmetry of the histogram. In several cases V_α is definitely larger than V_p (in more than 300 spectra the difference is greater than 10 percent), while only a few spectra give $V_\alpha/V_p < 0.9$. It is interesting to note that the frequency distribution of values of V_α/V_p given by *Robbins et al.* [1970] exhibits the same asymmetry as the HEOS 1 histogram. On the other hand, theories of the solar corona expansion [*Geiss et al.*, 1970; *Nakada*, 1970] do not suggest any mechanism of preferential acceleration of helium relative to the hydrogen component of the solar wind (see also the discussion by Geiss, p. 566).

The only experimental bias that could affect both the Vela and the HEOS histogram seems to be that when $V_\alpha < V_p$, detection of α-particles could sometimes be prevented by the higher proton fluxes; indeed, if $V_\alpha = 0.7V_p$, the α-particle peak in the energy per unit charge spectrum becomes coincident with the proton maximum and consequently cannot be observed. To evaluate the importance of the bias, we computed for each individual energy spectrum the lowest α-particle bulk velocity $V_{\alpha,min}$ that still could be resolved from the proton spectrum (that is, which would give an observable secondary peak) when no second peak for α-particles was observed. Such computations were performed assuming $W_\alpha = W_p$ and different values for the α-particle abundance (N_α/N_p). Results are shown in figure 2 in the form of frequency distributions of values

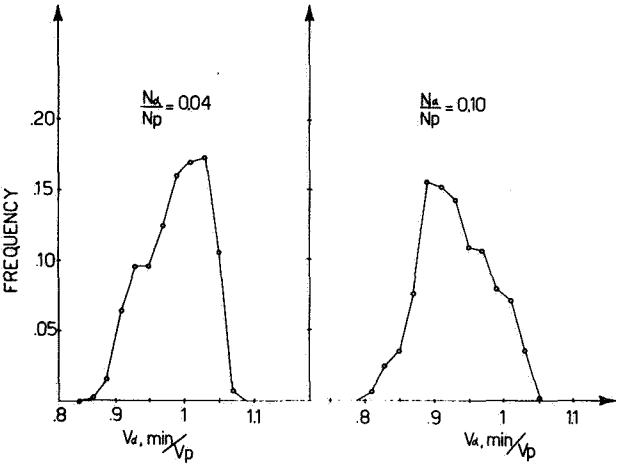

Figure 2. *Frequency distributions of values of $V_{\alpha,min}/V_p$ for two α-particle abundances. $V_{\alpha,min}$ is defined as the lowest α-particle bulk velocity which still could be resolved from protons (i.e., which would give an observable secondary peak in the energy per unit charge spectrum).*

of $V_{\alpha,min}/V_p$ for two values of the ratio N_α/N_p. As expected the bias decreases for high helium abundance, but it is certainly relevant for typical values of the ratio N_α/N_p (~0.05). The behavior of the average values of V_α and V_p versus N_α (fig. 3) confirms this result; in fact for $N_\alpha = 0.4$ cm^{-3}, $\overline{V_\alpha}$ reaches $\overline{V_p}$, becoming smaller than $\overline{V_p}$ for higher helium densities. It should be noted, however, that only a few spectra give $\overline{V_\alpha} < \overline{V_p}$. In figure 3 only cases with $|V_\alpha - V_p| > 20$ km/sec are considered consistent with detectability of a measurable difference between the two bulk velocities.

We can conclude that within the limitation of present experiments, no difference between the average bulk velocities of the two species is observed; however, an average $\overline{V_\alpha}$ lower than $\overline{V_p}$ would have not been observed. Deviations of the ratio V_α/V_p from 1 appear to be present during particular time periods.

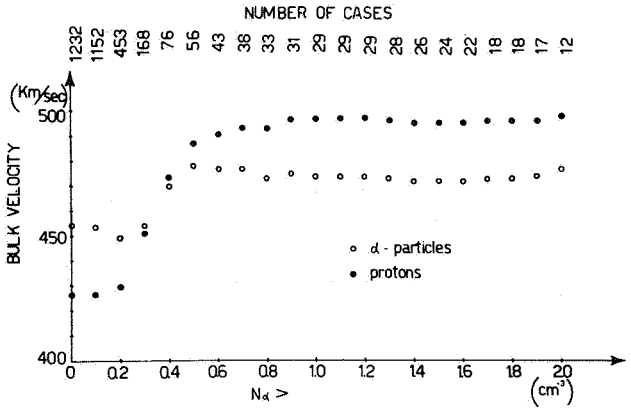

Figure 3. *Average values of V_α and V_p for N_α larger than given values. Only cases with $|V_\alpha - V_p| > 20$ km/sec have been considered.*

The frequency distribution of the relative abundances of helium is given in figure 4. The average value of the ratio N_α/N_p is 0.051. Figure 5 shows a time history of the helium abundance with the measured sunspot number taken as an index of solar activity. Values of N_α/N_p obtained by Vela 3 [*Robbins et al.*, 1970] and by Explorer 34 [*Ogilvie and Wilkerson*, 1969] are shown with HEOS 1 averages for comparison. Averages from HEOS 1 and Vela 3 satellites have been performed over

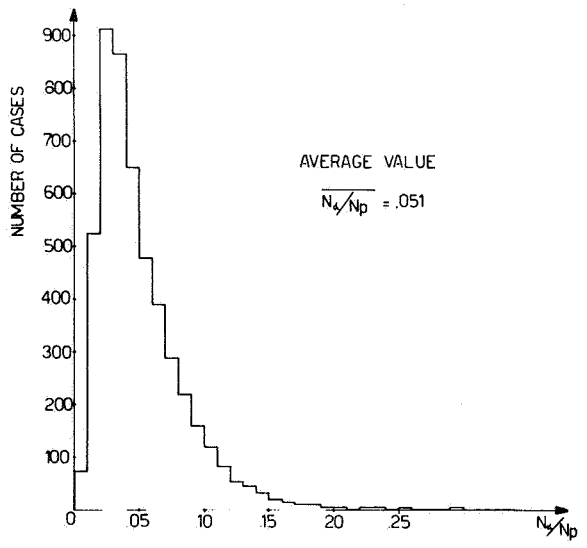

Figure 4. *Frequency distribution of individual values of N_α/N_p.*

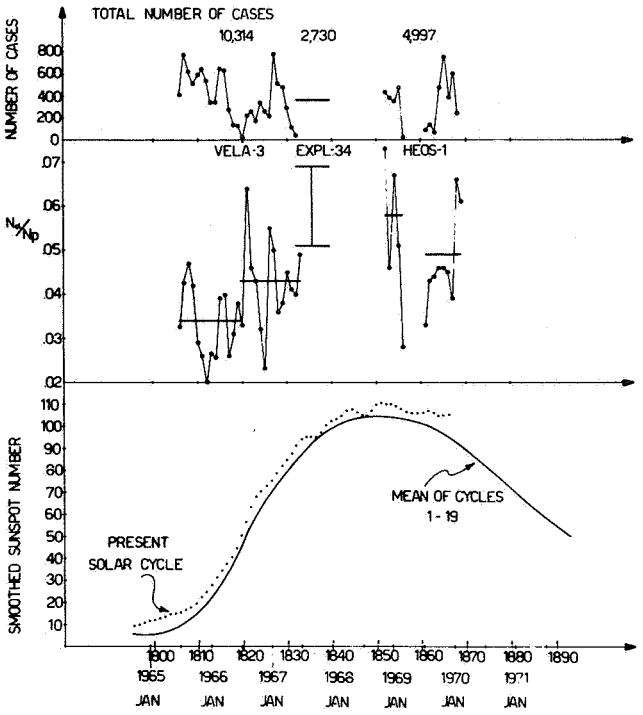

Figure 5. *Time history of the ratio N_α/N_p, according to observations performed by the satellites Vela 3, Explorer 34 and HEOS-1. Averages from HEOS-1 and Vela 3 [Robbins et al., 1970] have been performed over solar rotations (points) and over longer periods of time (bars). For Explorer 34 [Ogilvie and Wilkerson, 1969] only a total average is shown; the two values correspond to the average uncorrected for the instrumental bias (upper bar) and to the corrected average (lower bar). The number of cases over which the averages were performed is shown in the upper part of the figure. At the bottom, the measured sunspot number is given [Solar Geophysical Data, 1970].*

solar rotations (points) and over longer periods of time (bars). For Explorer 34 only a total average was available; the two values given in the figure correspond to the average uncorrected value (lower bar). The general pattern of the ratio N_α/N_p appears to confirm a dependence of helium abundance on the solar cycle.

The plasma bulk velocity appears correlated with the helium abundance. Figure 6 shows the average values of V_p and V_α computed over the spectra with N_α/N_p larger than 0.00, 0.01, 0.02, ... For the study of the steady-state condition of the solar wind, data referring to postshock periods (defined as 24 hr following a sudden

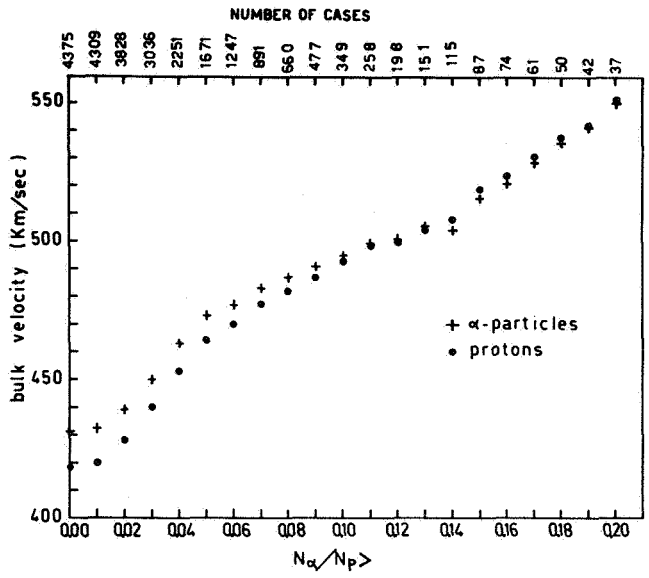

Figure 6. *Average values of V_p and V_α computed over the spectra with N_α/N_p larger than given values. The number of cases, over which the averages were performed, is shown on the top.*

commencement) have been removed from these averages. An increase of ~120 km/sec is observed in the bulk velocity of both species when N_α/N_p increases.

Figure 7 presents a comparison between the behavior of $\overline{V}_\alpha$, $\overline{V}_p$ versus N_α and $\overline{V}_p$ versus N_p. The $\overline{V}_p$ versus N_p plot, which was made with all the proton data (fig. 7(b)), shows the well-known result that the proton flux N_pV_p is approximately constant, in contrast to the general pattern of the $\overline{V}_\alpha$ versus N_α plot (fig. 7(a)), which shows a tendency to an increase of $\overline{V}_\alpha$ with N_α. Again it should be noted that for high densities of α-particles, $\overline{V}_\alpha$ becomes lower than $\overline{V}_p$.

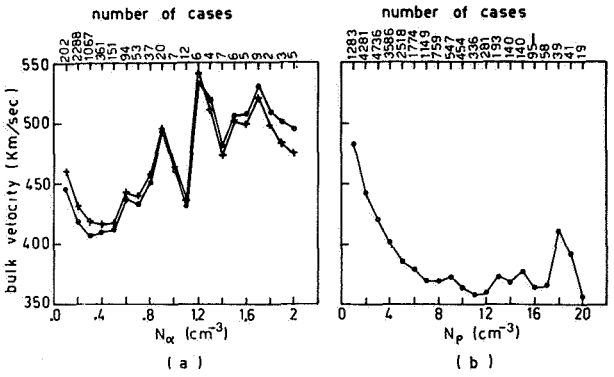

Figure 7. *Average values of $\overline{V}_\alpha$ and $\overline{V}_p$ plotted versus N_α (a) and of $\overline{V}_p$ versus N_p (b). Number of cases is given on top. The $\overline{V}_p$–N_p plot was made using all the available data.*

The increase in helium abundance together with the increase in the bulk velocity is predicted by the diffusion models of the solar corona [*Nakada*, 1970]. An increase in the coronal temperature, indeed, should increase the solar wind bulk velocity following the magnetohydrodynamic models [*Parker*, 1963; *Hartle and Sturrock*, 1968] and should also decrease the diffusion time, increasing the helium abundance in the expanding corona.

TWO-BEAM INSTABILITY

As shown in the previous section and by *Formisano et al.* [1970*b*] it is possible, occasionally, to observe different bulk velocities for protons and α-particles. Theoretically, it has been predicted [*Geiss et al.*, 1970; *Nakada*, 1970; *Yeh*, 1970; *Alloucherie*, 1970] that the helium bulk velocity should be lower (about 20 percent or more) than the proton bulk velocity in the solar corona, while some instability of the two stream type should be operating in the solar wind to equalize V_p and V_α. The problem has been studied with our data. The observations should reveal the quasi-steady state quickly reached by the solar wind at a few tenths of AU from the sun. Figure 8 shows the behavior of $\overline{W}_p$, $\overline{W}_\alpha$ versus V_α/V_p. The protons and helium average most probable thermal speeds increase for values of V_α and V_p different from 1. The observed variations of $\overline{W}_\alpha$ and $\overline{W}_p$ correspond to an increase of the proton and α-particle temperature of a factor 2. This result was already shown by *Formisano et al.* [1970*b*]. Figure 8 refers to more data, and the result is confirmed.

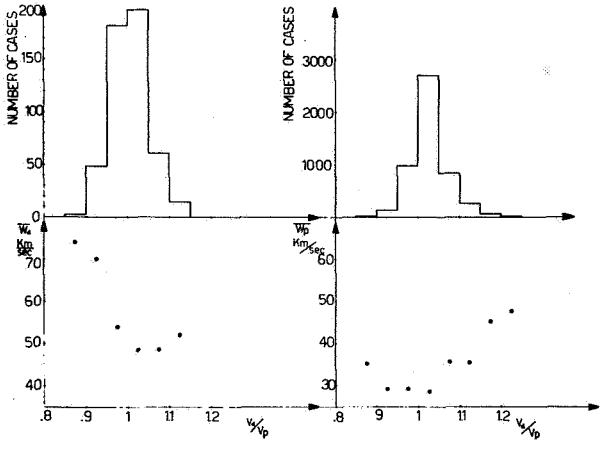

Figure 8. *Average values of W_α and W_p plotted versus V_α/V_p. Averages have been performed on V_α/V_p intervals of 0.05. In the upper part of the figure histograms of the total number of cases considered in the averages are given.*

The two-stream instability predicts that the faster beam will be slowed down, giving energy to waves and increasing the thermal energy of the particles. If the faster beam is the major beam—that is, has higher density (protons in the solar wind)—the energy available for waves and thermalization is large, and therefore a more rapid increase of the temperature of the slower beam and a higher noise level of unstable waves is expected. If the faster beam is the minor one (lower density, α-particles in the solar wind), a slower increase of the thermal energy of the slower beam is predicted. This behavior is shown in figure 8; $\overline{W}_\alpha$ increases faster (for $V_\alpha < V_p$) than $\overline{W}_p$ (for $V_\alpha > V_p$).

Figure 9 shows the actual solar wind points in relation to the two stream instability criterium of high frequency longitudinal waves for two maxwellian distributed beams [*Taylor*, 1970]. In a plane b,c $[b = 4(W_\alpha/W_p)^2$, $c = |V_\alpha - V_p|/W_p]$ plasma will be stable or unstable depending on the quantity $a = (N_\alpha/N_p)(W_p/W_\alpha)^3$. The stable region is the one on the left of the line corresponding to the given value of the parameter a.

Figure 9 shows for each (b, c) pair the edge of the stable region. The "a" scale is given at the top of the figure. All the data plotted have $|V_\alpha - V_p| > 10$ km/sec. All the points fall within the stable region, some just behind the stability line, most well inside the stable region. Lower values of $|V_\alpha - V_p|$ would give more points in the more highly stable region.

It should be remembered, however, that the two-streaming plasma is unstable with respect to both longitudinal and transverse waves. *Parker* [1961] has shown that Alfvén waves could be generated by a two-streaming plasma. *Kennel and Petschek* [1968] have related the firehose instability to the two-beam instability and the resulting instability criterium becomes

$$\beta\alpha_\alpha\alpha_p \left(\frac{V_\alpha - V_p}{W_p}\right)^2 + \Delta\beta \geq 2 \qquad (1)$$

where

$$\beta = \sum_{p,e,\alpha} \frac{3}{4}\frac{mW^2}{B^2/8\pi}$$

is the ratio between the total particle pressure and the magnetic pressure, $\alpha_p(\alpha_\alpha)$ is the ratio between the proton (α-particle) number density and the total ion number density; $\Delta\beta = \beta_\parallel - \beta_\perp$; $\beta_\parallel = 3\beta - 2\beta_\perp$; and $\beta_\parallel/\beta_\perp = K$ is the anisotropy ratio. It is evident from equation (1) that the firehose instability is modified if α-particles have $V_\alpha \neq V_p$ and that the difference $V_\alpha - V_p$ must be reduced by a firehose stable anisotropy in the three species. Figure 10 shows the stable region with respect to both firehose and two stream instability.

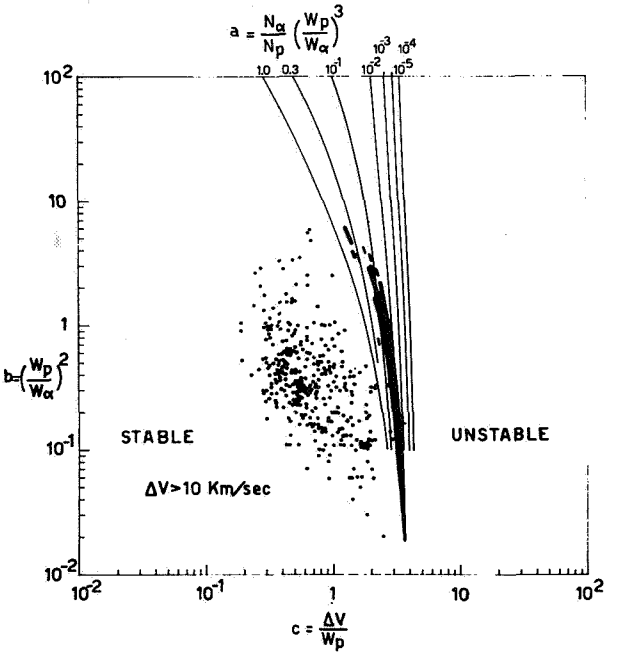

Figure 9. *The scatter plot of* $b = (W_p/W_\alpha)^2$ *and* $c = |V_\alpha - V_p|/W_p$. *The two-stream instability (for longitudinal waves) lines are shown for different values of the parameter* $a = N_\alpha/N_p\ (W_p/W_\alpha)^3$. *Black areas represent the edges of the stable region for each (b,c) pair.*

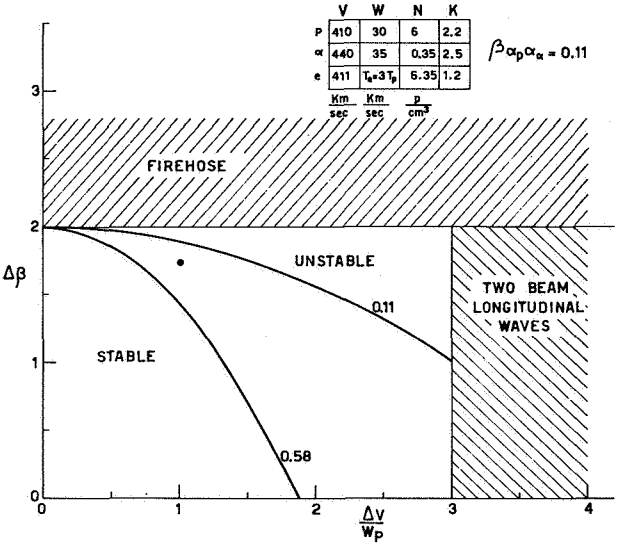

Figure 10. *Stability region with respect to the firehose and two stream instability. Equation (1) has been plotted for* $\beta\alpha_\alpha\alpha_p = 0.11$ *and 0.58. The 0.11 value refers to the set of parameters given on the top of the figure (the corresponding position in the* $\Delta\beta$, $\Delta V/W_p$ *plane is represented by the black point).*

As an example, a possible set of parameters and the corresponding position in the $\Delta\beta, \Delta V/W_p$ plane have been indicated.

It should also be noted that another instability, of the resonant type, has been found by *Barnes*, [1970] for bow shock reflected protons. It is not yet clear whether this instability can be important for the α-particle and proton streams.

SHOCK WAVE OBSERVATIONS

The behavior of α-particles through two interplanetary shock waves (February 28 and March 19, 1969) has been studied by *Formisano et al.* [1970*b*] using the HEOS 1 plasma data. Here we present the α-particle observations, together with interplanetary magnetic field measurements, during the two above-mentioned shocks and a third one, which occurred on March 25, 1969. This last event is discussed in detail by *Chao et al.* [1971].

Figure 11 shows the event, which occurred on February 28, 1969, detected at ground as a sudden commencement at UT 0425, by 19 stations. At UT 0422 a sudden increase of α-particle density, bulk velocity, and thermal speed is observed; V_α changes from 507 km/sec to 637 km/sec; N_α from 0.35 cm^{-3} to 0.80 cm^{-3}; W_α from less than 57 km/sec to ~88 km/sec.

The proton behavior is quite different: during about half an hour (from UT 0405 to UT 0431) V_p changes only ~50 km/sec. The proton density, which has an increment of ~30 percent at UT 0412, decreases to the previous value of 5 cm^{-3} when the α-particle discontinuity is detected. A small gradual increase is observed for the proton thermal speed. The proton energy spectrum, which was previously maxwellian, exhibits a non-maxwellian high-energy tail after the α-particle discontinuity, as had been shown by *Formisano et al.* [1970*b*]. The α-particle parameters show the characteristic variations of a shock. The identification of the α-particle discontinuity with a shock wave is confirmed by the magnetic field measurements. Indeed, simultaneously with the α-particle discontinuity, the magnetic field intensity increases of a factor 2 (from ~6γ to ~12γ).

Magnetic field oscillations are noted in the figure, before the sudden variation at UT 0422. They appear to be related to the earth's bow shock crossed by the satellite, moving outward from the earth, at UT 0120; during the 3-hr period from UT 0120 to UT 0422, these oscillations are permanently detected by HEOS 1, indicating the presence of waves associated with protons reflected from the earth's bow shock [*Asbridge et al.*, 1968].

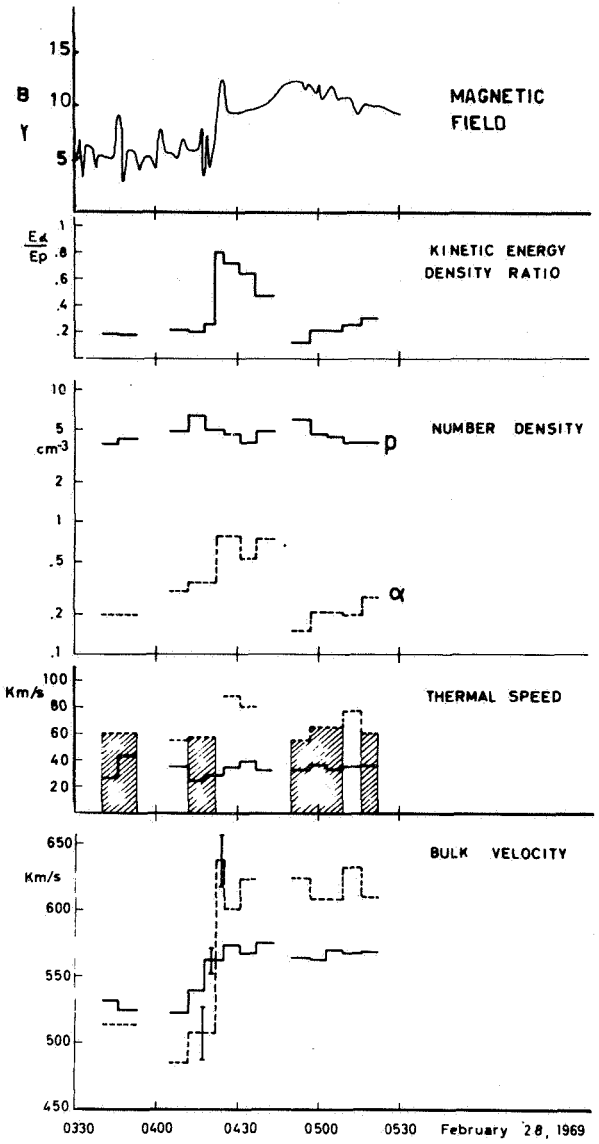

Figure 11. *Positive ion parameters and magnetic field for the event of February 28, 1969. From the top are given: the magnetic field intensity, the α-particle to proton kinetic energy density ratio; the α-particle and proton number densities; the most probable thermal speeds of protons and α-particles; the proton and α-particle bulk velocities. Broken lines refer to α-particles, continuous lines to protons.*

Figure 12 illustrates the March 19 event observed at ground as a sudden commencement at UT 1959. Three minutes before (at UT 1956 with an error of ±0.8 min) the protons exhibit a velocity discontinuity of ~45 km/sec (from 396 km/sec to 439 km/sec) and a

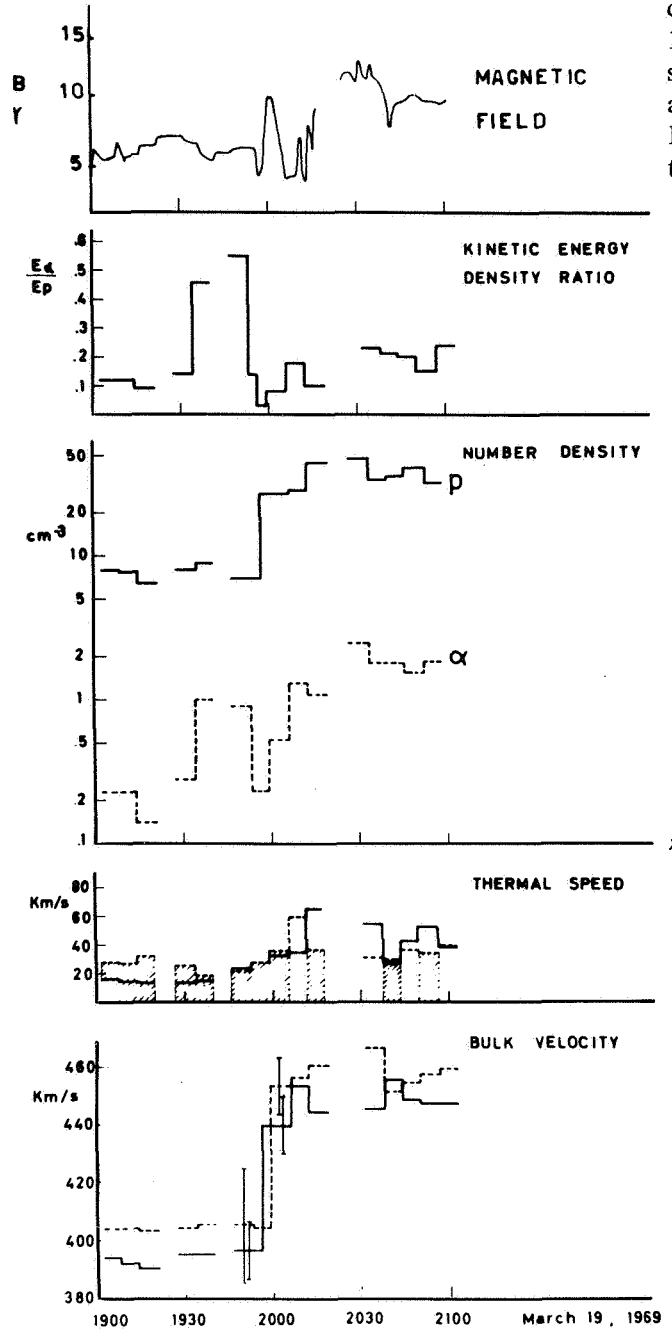

Figure 12. *Positive ion parameters and magnetic field intensity for the event of March 19, 1969.*

density increase by a factor of 4 (from 7 protons/cm^3 to 27 protons/cm^3), while the thermal speed increases by only 10 km/sec. The α-particle discontinuity (V_α from 404 km/sec to 453 km/sec and N_α from 0.2 cm^{-3} to 0.5 cm^{-3}) is observed with a time delay of ~3 min compared to the proton discontinuity [*Formisano et al.*, 1970*b*]. The magnetic field measurements show a sudden change of the field intensity (from ~5γ to ~10γ) at 1956 UT, simultaneously to the proton discontinuity. Later on, the magnetic field undergoes strong fluctuations.

Figure 13 illustrates the third shock wave occurring on

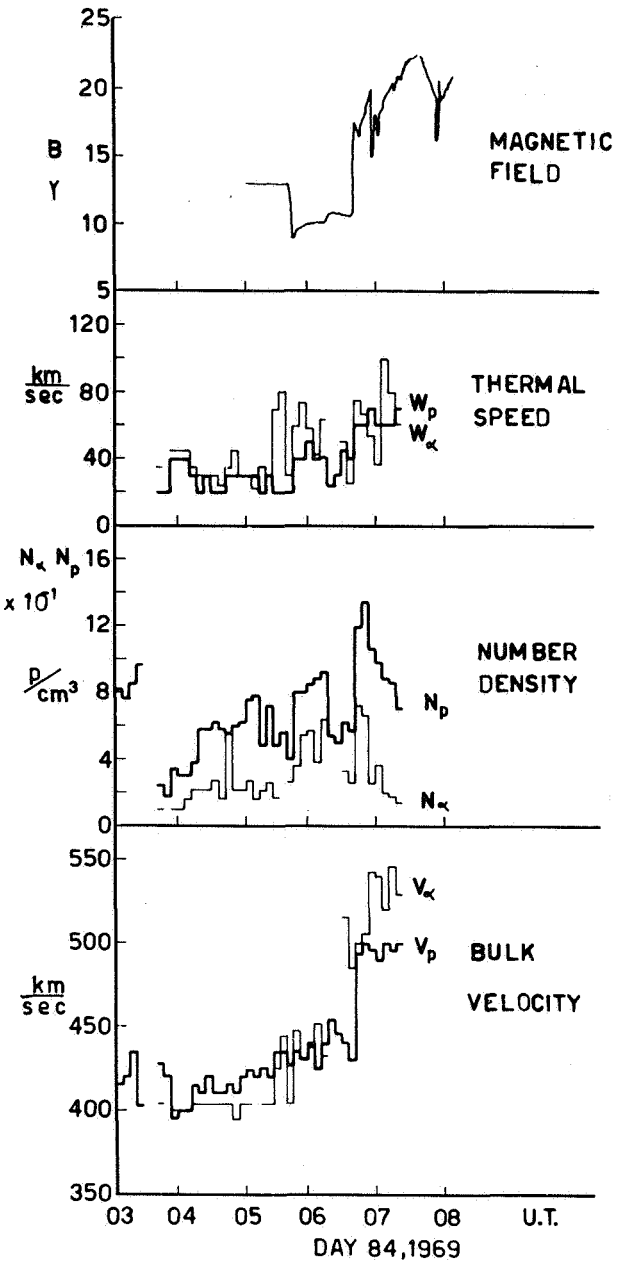

Figure 13. *Positive ion parameters and magnetic field intensity for the event of March 25, 1969. In the number density plot the scale of N_α should be multiplied by 10^{-1}.*

March 25. At UT 0646 a sudden variation of the proton parameters is observed (V_p from 435 km/sec to 490 km/sec; N_p from ~6 cm^{-3} to 10.4 cm^{-3}; W_p from 40 km/sec to 60 km/sec); at the same time, the magnetic field intensity increases from 10γ to 18γ. The α particles exhibit a different behavior. No relevant change of V_α is observed when the shock is detected, while a large discontinuity is observed a few minutes before the shock: V_α goes from 430 km/sec at UT 0614 to 515 km/sec at UT 0633 (two measurements are missed between).

Due to the data gap, we have no information on N_α at UT 0633, when the discontinuity of the α-particle bulk velocity is observed; however, the fact that α particles escape detection in the two subframes between UT 0614 and UT 0633 may suggest that N_α was lower during that period. When the proton shock is detected, at UT 0646, N_α increases from 0.3 cm^{-3} to 0.7 cm^{-3}.

The behavior of protons and α particles through the shock is better illustrated in figure 14. Three energy per unit charge spectra are shown: subframe 25630 is observed before the V_α change; subframe 25633 is observed just after the V_α increase, but before the proton discontinuity; subframe 25635 is taken just behind the shock. A maxwellian distribution was fitted to the three highest fluxes for both protons and α-particles; the obtained parameters are shown for both species. In all cases the maxwellian fits do not appear to be very good; in particular, a non-maxwellian high energy tail is clearly observed at UT 0633, when there was a large difference between proton and α-particle bulk velocities.

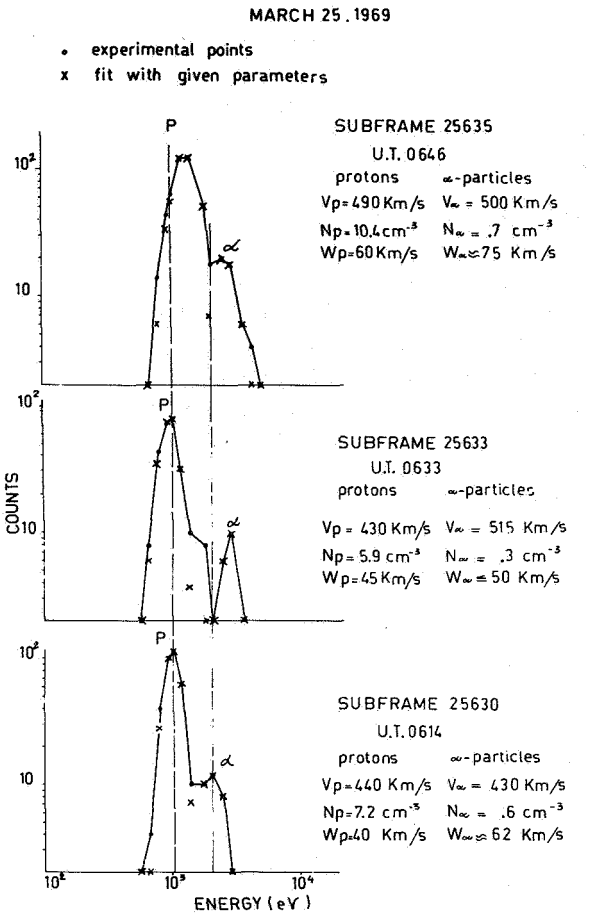

Figure 14. *Positive ion energy spectra observed on March 25, 1969, at UT 0614, 0633 and 0646. Electrometer counts (black points) are plotted versus energy per unit charge. P indicates proton peaks; α indicates α-particle peaks. Crosses indicate the maxwellian fit of the observed spectra for the given values of proton and α-particle parameters.*

CONCLUSIONS

We can summarize our results as follows:

1. Within the limitations of present experiments, no difference between the average bulk velocities of protons and α-particles is detected. However, due to an instrumental bias, the possibility of V_α being lower than V_p cannot be ruled out.
2. Data from the satellites Vela 3, Explorer 34, and HEOS 1 give evidence of a dependence of helium abundance on the solar cycle.
3. On average, high helium abundances are observed together with high bulk velocities, in agreement with diffusion models of the solar corona.
4. When a definite difference between proton and α-particle bulk velocity is observed, the stability with respect to high frequency longitudinal waves is ensured by higher thermal speeds. However, the problem of transverse wave instability, due to differences between V_α and V_p, has not been investigated.
5. The behavior of α-particles through interplanetary shock waves is not a simple one. Strong discontinuities may be observed in one species, without occurring in the other, or having different characteristics. In particular, the magnetic field observations confirm the interpretation of the α-particle discontinuity, occurred on February 28, 1969, as a shock wave.
6. When a strong discontinuity is detected only for α-particles, the proton distribution function shows a large non-maxwellian high-energy tail.

ACKNOWLEDGMENTS

We are very grateful to Prof. A. Egidi for useful discussions. We are indebted to the other personnel of the

Laboratorio per il Plasma nello Spazio of Rome who have participated in the development of the solar wind experiment. This research has been supported by the Consiglio Nazionale delle Ricerche of Italy. The HEOS 1 magnetic field experiment was supported by the British Science Research Council.

REFERENCES

Alloucherie, Y.: Diffusion of Heavy Ions in the Solar Corona. *J. Geophys. Res.*, Vol. 75, 1970, p. 6899.

Asbridge, J. R.; Bame, S. J.; and Strong, I. S.: Outward Flow of Protons from the Earth's Bow Shock. *J. Geophys. Res.*, Vol. 73, 1968, p. 5777.

Barnes, A.: Theory of Generation of Bow Shock Associated Hydromagnetic Waves in the Upstream Interplanetary Medium. *Cosmic Electrodyn.*, Vol. 1, 1970, p. 90.

Bonetti, A.; Moreno, G.; Cantarano, S.; Egidi, A.; Marconero, R.; Palutan, F.; and Pizzella, G.: Solar Wind Observations with the ESRO Satellite HEOS 1 in December 1968. *Nuovo Cimento B*, Vol. 64, 1969, p. 307.

Chao, J. K.; Formisano, V.; and Hedgecock, P. C.: Shock Pair Observation in the Solar Wind. Preprint, 1971.

Formisano, V.; Egidi, A.; and Moreno, G.: Observations of Solar Wind α-Particles in the Magnetosheath. *Lettere Nuovo Cimento*, Vol. 3, 1970*a*, p. 209.

Formisano, V.; Moreno, G.; and Palmiotto, F.: α-Particle Observations in the Solar Wind. *Solar Phys.*, Vol. 15, 1970*b*, p. 479.

Geiss, J.; Hirt, P.; and Leutwyler, H.: On Acceleration and Motion of Ions in Corona and Solar Wind. *Solar Phys.*, Vol. 12, 1970, p. 458.

Hartle, R. E.; and Sturrock, P. A.: Two Fluid Model of the Solar Wind. *Astrophys. J.*, Vol. 151, 1968, p. 1155.

Hedgecock, P. C.: The Solar Particle Event of February 25, 1969. *Intercorrelated Satellite Observations Related to Solar Events*, edited by V. Manno and D. E. Page. D. Reidel, Dordrecht-Holland, 1970, p. 419.

Kennel, C. F.; and Petschek, H. E.: Magnetic Turbulence in Shocks. *Physics of the Magnetosphere*, edited by R. L. Carovillano, J. F. McClay, H. R. Radoski. D. Reidel, Dordrecht-Holland, 1968.

Nakada, M. P.: A Study of the Composition of the Solar Corona and Solar Wind. *Solar Phys.*, Vol. 14, 1970, p. 457.

Ogilvie, K. W.; and Wilkerson, J. D.: Helium Abundance in the Solar Wind. *Solar Phys.*, Vol. 8, 1969, p. 435.

Parker, E. N.: A Quasi Linear Model of Plasma Shock Structure in a Longitudinal Magnetic Field. *J. Nucl. Energy C2*, 1961, p. 146.

Parker, E. N.: *Interplanetary Dynamical Processes.* Interscience, New York, 1963.

Robbins, D. E.; Hundhausen, A. J.; and Bame, S. J.: Helium in the Solar Wind. *J. Geophys. Res.*, Vol. 75, 1970, p. 1178.

Solar Geophysical Data, U.S. Department of Commerce, Washington, D.C., Sept., 1970.

Taylor, I.: Penrose Criterion for Multistreaming Maxwellians, ESRIN Internal Note N.74, Feb. 1970.

Yeh, T.: A Three Fluid Model of Solar Wind. *Planet. Space Sci.*, Vol. 18, 1970, p. 199.

DISCUSSION

J. Hirshberg Remarking on the helium abundance increasing as the solar cycle goes on, I compared your data with the Vela data and it seems that in those two samples the most probable value remained stationary. What happened was that as the solar cycle progressed you obtained more high helium observations which would be consistent with the notion that enhanced helium was coming out of flares.

G. Moreno That's right, the modal value was the same in two cases, only the enhanced helium changed. I forgot to say that the correlation of the bulk velocity of both protons and α particles bulk velocity with the helium abundance has been done only for quiet periods.

M. Dryer How many energy channels do you have in your analyzer?

G. Moreno Twenty-eight. Computation suggests that the velocity spread from one channel to the next error in velocity is perhaps less than 20 km; in many cases when α particles are in three channels it becomes much less.

D. Heymann Several years ago, as you well know, it was suggested by Dr. Michel that a tenuous atmosphere on the moon is removed by the interaction of this atmosphere with the solar wind rather than by gravitational escape. ^{40}A was not removed from the moon but was punched back into the lunar surface by essentially the same mechanism

that Michel proposed for the escape of neutral atoms, i.e., via ionization then acceleration in the interplanetary electric and magnetic field from the moon. The ^{36}A, as he argued, varies quite a bit, but it varies because it is surface correlated. He argued and showed that all the ^{36}A is essentially from the solar wind, and implanted in the surface of these particles. Now, the curious thing is that when we measured ^{40}A in the same particles they correlate, I mean, they co-vary with ^{36}A. And in fact $^{40}A/^{36}A$ in these samples is about unity; that is a paradox because all theoreticians tell us that $^{40}A/^{36}A$ in the sun ought to be much less than unity, in fact perhaps much lower than 10^{-4}. So the question is where the ^{40}A that we are seeing in the samples comes from. It cannot come from the solar wind proper. You may wonder and say perhaps this ^{40}A has arisen from ^{40}K decay in these samples and what we note is simply that these samples are low in ^{40}K or have a young age or both, and that these samples have much potassium or have an old age or both. But that cannot be true because for any of these points if you calculate an honest $^{40}K/^{40}A$ age you find that all the ages are greater than the accepted age of the moon and in fact calculate ages greater than $7X10^9$ yr. So the ^{40}A has been produced from potassium not in these samples but somewhere else, has been separated, and then reimplanted into the lunar regolith. In other words, what we are looking at is Argon which was produced in the body of the moon, by potassium decay, was made available in the lunar atmosphere. You can, for example, envisage Argon just oozing out slowly. It might be that there were large impacts on the surface of the moon which threw out vast amounts of rock and that Argon was subsequently reimplanted—being coupled to the solar wind which is the driving agent of this reimplantation into the soil—and that is basically the reason we see the covariation of ^{40}A and ^{36}A.